AAPS PharmSciTech **2003; 4 (4) Article 67 (http://www.aapspharmscitech.org).**

Thermal Porosity Analysis of Croscarmellose Sodium and Sodium Starch Glycolate by Differential Scanning Calorimetry

Submitted: July 7, 2003; Accepted: November 4, 2003

Damrongsak Faroongsarng[1] and Garnet E. Peck[2]

[1]Department of Pharmaceutical Technology, Faculty of Pharmaceutical Sciences, Prince of Songkla University, Hat Yai, Songkhla, Thailand 90112

[2]Department of Industrial and Physical Pharmacy, School of Pharmacy, Purdue University, West Lafayette, IN 47907-2012

ABSTRACT

The aim of the study was to demonstrate the applicability of differential scanning calorimetry (DSC) on porosity analysis for cellulose and starch. Croscarmellose sodium (CCS) and sodium starch glycolate (SSG) were allowed to sorb moisture in 85%, 90%, 95%, and 100% relative humidity (RH) at 40°C for 24 hours. The pretreated samples were then subjected to DSC running temperature ranging from 25°C to -50°C at a cooling rate of 10°C/min. The cooling traces of water crystallization, if present, were transformed to porosity distribution via capillary condensation using Kelvin's equation. The porosity analysis of CCS and SSG was also done using nitrogen adsorption as a reference method. It was found that sorbed water could not be frozen (in cases of 85% and 90% RH) until the moisture content exceeded a cutoff value (in cases of 95% and 100% RH). The nonfreezable moisture content was referred to tightly bound, plasticizing water, whereas the frozen one may be attributed to loosely bound water condensation in pore structure of CCS and SSG surfaces. Not only capillary condensation but also the tightly bound, nonfreezable monolayer water lying along the inner pores of the surface contributed to porosity determination. Good agreement with less than 5% deviation of mean pore size was observed when the results were compared with nitrogen adsorption. The narrower pore size distributions, however, were obtained because of the limitations of the technique. It was concluded that pore analysis by DSC could be successful. Further research needs to be done to account for limitations and to extend the applicability of the technique.

Corresponding Author: Damrongsak Faroongsarng, Department of Pharmaceutical Technology, Faculty of Pharmaceutical Sciences, Prince of Songkla University, Hat Yai, Songkhla, Thailand 90112; Tel: +66-74-288-841; +66-74-428-148; Email: fdamrong@ratree.psu.ac.th

KEYWORDS: thermoporometry, differential scanning calorimetry (DSC), croscarmellose sodium (CCS), sodium starch glycolate (SSG)

INTRODUCTION

It has been long recognized that water vapor adsorbs on the hydrophilic surface mainly because of hydrogen bonding.[1] Sorbed water presents thermodynamic properties somewhat different from bulk water. For instance, sorbed water is able to crystallize at a temperature considerably lower than 0°C and presents in 2 forms: nonfreezable and freezable.[2] Earlier investigators[1] suggested at least 2 forms of sorbed water including specific site-interaction water, and water condensation in the pore structure of sorbent. Later, Zografi and Kontny[3] stated that water exists in at least 3 thermodynamic states: (1) water directly and tightly bound; (2) water in a relatively unrestricted form, approaching the properties of bulk water; and (3) water in an intermediate state, with properties reflecting a higher level of structure than bulk water but less than that of tightly bound. On one hand, it was proposed that specific site-interaction water was located on the glassy amorphous region[4] of polymer sorbents and could not be frozen.[5] This was referred to directly and tightly bound water that present in interpolymer molecular space. Water molecules acted as a plasticizer causing a lowering of the glass transition temperature of polymer sorbents.[6] On the other hand, water condensation occurred because the surface of condensed water in the pore structure is concave and its vapor pressure is smaller than its saturation pressure.[7] It was referred to water in essentially unrestricted form and could be frozen.

The chemical nature of the materials played an important role since the water sorption was not mainly physical adsorption, but specific interaction. To examine the nonfreezable/freezable bound water, the very hygroscopic materials were subjected to vapor sorption study. It had been claimed that both celluloses and starches possess surface

hydroxyls as the interaction sites for water via hydrogen bonding.[1] Two of the cellulose and starch derivatives, so-called commercially available superdisintegrants including croscarmellose sodium (CCS) and sodium starch glycolate (SSG), were selected. CCS is a cross-linked product of carboxymethyl cellulose, whereas SSG is a low-substituted derivative of potato starch obtained by cross-linking and carboxymethylating. These 2 products have been reported to sorb moisture approximately 40% to 50% by weight when subjected to a very high relative humidity (RH) environment.[8]

Not only the states of bound water but also capillary condensation[9] can be attributed to strong water-hydrophilic site interactions.[10] Furthermore, the condensed water in the pore structure on surfaces could develop the driving force that makes water diffuse into the bulk.[11] Using the model proposed by the investigators who formulated this hypothesis, it was found that the sorbed moisture tended to be on the CCS or SSG surface (adsorption) as a normally condensed phase, rather than diffusing into the bulk (absorption).[6] The evidence then suggested the possibility of using frozen water of sorption on CCS and SSG for porosity determination.

Powder pore analysis has currently been done by gaseous adsorption. There are limitations of this method as it requires a number of steps including outgasing, step-by-step equilibrating with different relative pressures, and measuring volume of gas adsorption at corresponding relative pressure. This method is time consuming especially with highly porous materials since a considerably long time has to be allowed to equilibrate the sample. DSC provides considerably fewer steps, is less time consuming, and is less expensive. In addition, it has been claimed that thermoporometry has the potential for determination of the pore size distribution over a wider range of pore size than the nitrogen gas adsorption-desorption method.[12]

An attempt to accomplish pore analysis by the DSC method has been made previously, but only an empirical approach was utilized.[9,12-14] The objective of this study was to demonstrate the applicability of frozen bound water sorbed on 2 hydrophilic polymers, namely, CCS and SSG, that can be detected by DSC for porosity analysis. The capillary condensation phenomenological described by Kelvin equation, rather than the approach of previous works, was used.

Thermoporometry of Water Vapor Sorbed on Hydrophilic Polymer

The hypothesis of freezable bound water capillary condensation leads to thermal porosity analysis utilizing water crystallization data via partial thermodynamic quantities described as follows:

Thermoporometry is based on the principle of freezing (or melting) point depression, which is due to strong curvature of the solid-liquid interface present within pores.[9] The relationship between the radius of the water-filled pores and the condensation pressure is described by the Kelvin equation[15]:

$$ln\frac{p}{p_0} = -\frac{2\gamma V_l}{r_k RT}cos\Theta \qquad (1)$$

where, p is pressure across the curvature subjected to be the Kelvin's radius of cylindrical pore, r_k, relative to an equilibrium vapor pressure of the same liquid on the plane surface (p_0). V_l and γ are molar volume (18 cm^3/mol) and surface tension (1.72×10^{-6} cal/cm^2) of liquid water, respectively. θ is the contact angle between inner pore surface and liquid meniscus. R and T are gas constant and absolute temperature, respectively. Since condensation and evaporation are in equilibrium, the finite change in free energy during the process described by the partial Gibb's free energy: $\Delta\overline{G} = RT\,ln\frac{p}{p_0}$ for complete wetting, where θ is zero and its cosine is equal to 1, is presented as Equation 2.

$$\Delta\overline{G} = -\frac{2\gamma V_l}{r_k} \qquad (2)$$

Partial thermodynamic quantities of freezable bound water assumed to be attributed to capillary condensation for each of the samples were calculated based on the concept of relative activities between the liquid-solid transition, where the quantities are assumed to be directly dependent upon heat of crystallization:

$$a_l = 1 - \frac{A_l}{A_T} \qquad (3)$$

where a_I, A_I, and A_T are activity of the liquid water at corresponding temperature, partial area under the DSC cooling trace at a temperature where activity of the liquid water present, and total area, respectively. The activity of ice is set to 1. The partial enthalpy change ($\Delta\overline{H_l}$) and partial entropy change ($\Delta\overline{S_l}$) of the condensed liquid water at corresponding temperature (T) are calculated using Equations 4 and 5,[16] respectively.

$$\Delta\overline{H_l} = -R\cdot T^2\left(\frac{\delta ln a_l}{\delta T}\right)_p \qquad (4)$$

$$\Delta \overline{S}_l = -R \cdot [\frac{\delta(T \cdot ln\, a_l)}{\delta T}]_p \quad (5)$$

Partial Gibb's free energy change ($\Delta \overline{G_l}$) was then calculated as follows:

$$\Delta \overline{G}_l = \Delta \overline{H}_l - T \cdot \Delta \overline{S}_l \quad (6)$$

From Equations 2 and 6, the information of partial Gibb's free energy could be transformed to Kelvin's radii of porosity system. In addition to the radii, should an assumption of linear relationship between mass and heat of water crystallization be made, one could get the information of porosity distribution of system under study.

In addition, the equation dealing with freezing point depression has been known as van't Hoff law, showed by Equation 7.[17]

$$ln\left[\frac{a_s}{a_l}\right] = \frac{\Delta H_0}{R T_0 T_m} \cdot \Delta T \quad (7)$$

Notations *l* and *s* refer to liquid water and ice, respectively. Where ΔH_0, T_0, T_m, and ΔT are molar heat of fusion, freezing point of pure water, freezing point of sorbed water, and freezing point depression (ie, T_0-T_m), respectively. It is noted that the activity of liquid (a_l)-solid water (a_s) is converted to partial Gibb's free energy via the relationship $\Delta \overline{G_l} = -RT\, ln \frac{a_s}{a_l}$. From Equations 2 and 7, The relationship between Kelvin radius and freezing point depression yields:

$$r_k = \frac{2\gamma V_l \cdot T_m}{\Delta H_0 \cdot \Delta T} \quad (8)$$

which leads to the equation used for transformation of the abscissa of the DSC curve to the pore radius (r) with empirical functions of freezable-Kelvin's radius and thickness of non-freezable layer, $\alpha(T)$ and β, respectively, proposed previously by a number of authors[12-14]:

$$r = \frac{\alpha(T)}{\Delta T} + \beta \quad (9)$$

Thus, it is clearly seen that $\alpha(T)/\Delta T$ in Equation 9 is equivalent to r_k in Equation 8, whereas β is a correction term for nonfreezable layer. The approach used in the study is a phenomenological alternative to the previous method of thermoporosity determination.

MATERIALS AND METHODS

Two hydrophilic polymers, namely, CCS (Ac-di-sol, FMC Corp, Philadelphia, PA) and SSG (Primojel, Generichem Corp, Little Falls, NJ) were employed. The results from previous work[8] suggested that, kinetically, CCS and SSG sorbed moisture in apparent first-order fashion. In both cases, the amount of sorbed water in grams reached a plateau level by 24 hours of equilibration. Each of the materials was equilibrated in 100%, 95%, 90%, and 85% RH chambers provided by different aqueous concentrations of sodium hydroxide at 40°C ± 2°C for 24 hours prior to DSC study. Hydranol composite-2 Karl Fisher reagent (Riedel-deHaen, Hoechst Celanase Corp, Charlotte, NC) and methanol were used for equilibrium water content determination (Metrohm 701 KF titrino, Brinkmann Instrument Inc, Westbury, NY).

Each of accurately weighed pretreated samples (5-10 mg) was placed in volatile DSC pan and tightly sealed. To examine frozen or nonfrozen sorbed water for each of the samples, the exotherm (cooling trace) was obtained by DSC study (DSC-7, Perkin Elmer Corp, Norwalk, CT); temperature ranged from 25°C to -50°C at a cooling rate of 10°C/min. The DSC pan filled with liquid water was also run using the identical conditions as a positive control.

The obtained exotherms, in which the water crystallization trace was revealed, were numerically treated to determine the partial thermodynamic quantities as described in Equations 4 to 6. The partial Gibb's free energies were then transformed to Kelvin's radii by Equation 2. The porosity distribution was then characterized by nonlinear fitting using logarithmic-normal model. The DSC information was exported from Pyris software (Perkin Elmer Corp, Norwalk, CT) to an MS Excel spreadsheet (Excel 97, Version 8.0, Microsoft Corp, Redmond, WA) prior to numerical calculation. All of the calculations were done by in-house computer software on a PC.

The nitrogen adsorption method was also employed to determine porosity distribution of each of the materials. Accurately weighed powder samples were outgased for 24 hours at 70°C to rid them of surface moisture and other contaminants. The sample was then subjected to the automatic surface area analyzer (Autosorb-1, Quantachrome, Syosset, NJ). The materials' powder nitrogen adsorption isotherms were obtained at 77 K. The pore size distribution was calculated according to Kelvin equation with a method based on the area of the pore walls.[18]

RESULTS AND DISCUSSION

Figures 1 and **2** respectively illustrate the DSC exotherms of CCS and SSG previously equilibrated with various hu-

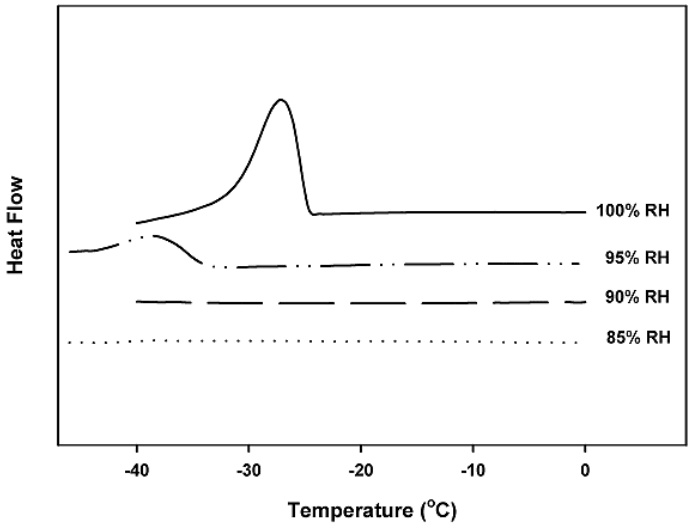

Figure 1. DSC exotherms (cooling traces) of CCS equilibrated with 100%, 95%, 90%, and 85% RH environments.

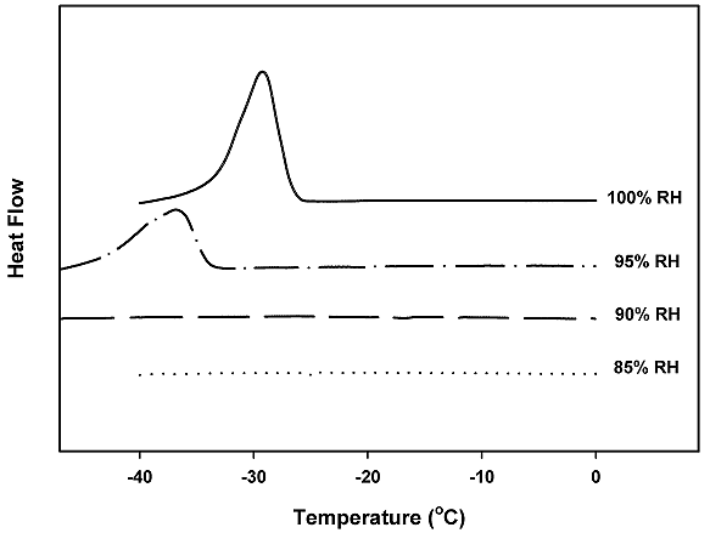

Figure 2. DSC exotherms (cooling traces) of SSG equilibrated with 100%, 95%, 90%, and 85% RH environments.

Table 1. Water Crystallization Temperature and Equilibrium Moisture Content of Croscarmellose Sodium and Sodium Starch Glycolate Equilibrated With Different Relative Humidities*

	CCS		SSG	
Humidity	T_0 (°C)	**EMC (% wt/wt)**	T_0 (°C)	**EMC (% wt/wt)**
85% RH	†	26.8	†	30.9
90% RH	†	31.3	†	37.1
95% RH	–40.1	38.8	–38.0	50.1
100% RH	–27.7	50.2	–29.7	74.8

*CCS indicates croscarmellose sodium; EMC, equilibrium moisture content; RH, relative humidity; SSG, sodium starch glycolate; and T_0, water crystallization temperature °C. With the identical conditions, the temperature of bulk water crystallization was –23.7°C, which was far below zero because the DSC experiment was carried out with nonequilibrium manner.
†nonfreezable

midity environments, and **Table 1** shows the temperatures of water crystallization as well as their equilibrium moisture contents (EMC). The results suggested that at less than 90% RH, up to 30% to 40% wt/wt of water sorbed on CCS and SSG could not be frozen. Previous study demonstrated that part of water sorbed on polyvinyl alcohol (PVA), an example of hydrophilic polymer, begins to crystallize only when the water content is above a characteristic threshold.[19] It is deduced to be a cutoff between tightly associated and bulk-sorbed water. The cutoff moisture contents in cellulose and starch systems were previously reported to be 18% and 30% wt/wt, respectively.[8] It was projected that the cutoff EMC of CCS was higher, whereas that of SSG was comparable (**Table 1**). Unlike starch, which mostly presents as amorphous form, cellulose is partial crystalline. The crystalline portion has been eliminated during the CCS manufacturing process making its morphology to be amorphous, and consequently increasing sorption sites.[4] Thus, the portion of tightly bound water was increased.

It was found that upon cooling, for the high humidity environments, the ice formation began at a temperature far below that of bulk water (**Table 1**) because of crystallization difficulty. Moreover, the relative content between nonfrozen and frozen water seemed to effect crystallization temperature. As seen in **Table 1**, when there was less relative portion of non-freezable/freezable bound water, the temperature was higher. The interaction between water molecule and a functional site may be strong enough to prevent the formation of ice crystal in cases of within the cutoff moisture content. On the other hand, in cases of high moisture content that exceeds the cutoff EMC, with a role of hydrogen bonding between water molecules, the concave surface of condensed water, and its lower-than-saturation vapor pressure, water undergoes condensation in the porosity of the sample.[7]

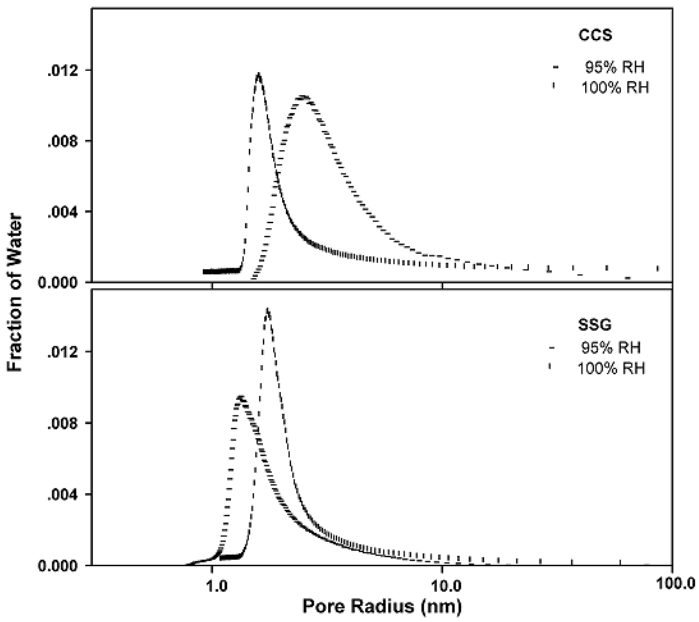

Figure 3. The porosity distribution of CCS (above) and SSG (below) obtained from DSC exotherms via Kelvin equation and partial thermodynamic quantities. Vertical rods indicate samples equilibrated with 100% RH. Horizontal rods indicate samples equilibrated with 95% RH.

The free, loosely bound, or weakly or nonplasticizing water thus can be seen from DSC freezing. Water-polymer interaction and its hydrogen bonding between water molecules themselves may govern the crystallization process causing the variability in position and shape of the <0°C freezing traces. In humidity as high as 100%, water first sorbed at sites on the glassy amorphous region of the polymer. Sorbed water, in turn, acted as the plasticizer causing the loss of glassy regions (ie, consequent decrease in sites of consecutive sorption). Upon cooling, condensed-phase water crystallization formed more easily with higher freezing point and appeared slightly sharper in shape (**Table 1** and **Figures 1-2**) compared with that of 95% RH.

The exotherms of freezable bound water sorbed on CCS and SSG at 95% and 100% equilibrated humidity environments were transformed to porosity distributions seen in **Figure 3**. Pore sizes and their distributions were determined by a logarithmic normal distribution model and tabulated in **Table 2**. As seen in **Figure 3** and **Table 2**, the porosity obtained was in the range classified as mesopores.[18] The porosity distribution width for individual samples in 95% RH was broader compared with that in 100% RH. This was reflected from DSC exo-therms discussed above. In other words, it may be deduced that the effect of more water-polymer interaction due to less loss of consecutive sorption sites, in the case of 95% RH, against hydrogen bonding between water molecules encounter the difficulty in capillary condensation. In consequence, the partial pore filling might result. Westermarck[20] described that the Kelvin's pore radius of aqueous capillary condensation may be valid only in the range from approximately 1.8 to 30 nm. The ranges of Kelvin's radii obtained from partial Gibb's free energy in this study just lie along the lower boundary of Westermark's statement. One of them (ie, SSG equilibrated with 95% RH) might be outside the range (**Table 2**). However, previous thermoporometric study determined average pore radius of a silica sample as low as 1.6 nm.[16] Fortunately, the results were comparable with what was determined by nitrogen adsorption method. To be sufficiently confident, the population of radii obtained in cases of 100% RH equilibration were chosen where the data were not away from the previously proposed valid range.

Table 3 shows the characteristic porosity distribution obtained from nitrogen adsorption utilizing a technique of the area of the pore walls.[18] The nitrogen adsorption has been an established standard method for specific surface determination and pore analysis for several years.[18] Should it be taken as a reference, it was found then that the pore size obtained from partial Gibb's free energy illustrated a bias estimation compared with the nitrogen adsorption method.

The fact is that the radii obtained from capillary condensation in surface pore structure were derived from freezable bound water only. The obtained Kelvin's radii should be "core-" rather than "pore-"radii because as a result of bound water that could not be frozen, there is a thickness that lies along the surface of the inner pores (eg, β-parameter in Equation 9). The thickness of the layer of nonfreezable pore water determined via thermoporosity (ie, β-parameter) of silica gels was reported that corresponded to 1 to 3 folds of water monolayer with the average value of 1.4.[16] Considering a stronger water-functional site interaction, it is thus assumed that the thickness of nonfreezable water be in a range of a monolayer. In addition, previous study demonstrated that the mean particle sizes of CCS and SSG dispersed in water increased by 1.6- and 4.4-fold, respectively.[8] The consequent swelling due to hydration may take place in these cases since it is assumed that bound water behaves as a liquid-like state. The molecular diameter of water is .28 to .3 nm.[21] If the nonfreezable bound water is able to cause polymer swelling, the monolayer thickness (β) is then calculated as follows:

$$\beta = f_S \times \sigma \qquad (10)$$

where f_s is the swelling factor (1.6 and 4.4 for CCS and SSG, respectively) and σ is the molecular diameter of water (.29 nm). **Table 3** also illustrates the adjusted mean pore radii on the surface of CCS and SSG from partial Gibb's free energy with 100% RH equilibration compared

Table 2. The Characteristics of Porosity Distributions of Study Materials Equilibrated With 95% and 100% Relative Humidity Obtained From Water Capillary Condensation*

Material With RH	Mean Radius† $\overline{r_k}$ (nm)	Distribution Width‡ (nm)	95% Radii Population Range§	R‡
CCS with 95% RH	2.68 (0.020)	.211	1.56-4.59	0.9326
CCS with 100% RH	1.67 (0.005)	.202	1.34-2.08	0.9312
SSG with 95% RH	1.44 (0.006)	.203	1.05-1.98	0.9365
SSG with 100% RH	1.82 (0.005)	.201	1.46-2.27	0.9652

*CCS indicates croscarmellose sodium; RH, relative humidity; and SSG, sodium starch glycolate.
‡Correlation coefficient of nonlinear fitting based on the model

$f = A \cdot exp\left[-0.5(ln\frac{r}{r_k})/b)^2\right]$, where $\overline{r_k}$ and b are mean size of Kelvin's radius and the logarithmic value of distribution half-width, respectively.

The distribution width is the value of exp(-b) + exp(+b).
†Mean size was reported in nanometers (nm) with standard error of fitting presented in the following parentheses.
§Taking as logarithmic-normal distribution, the limits of 95% population range can be calculated as $exp\left[ln(\overline{r_k}) \pm Z_{0.95} \cdot b\right]$.

Table 3. Porosity Analyses of Croscarmellose Sodium and Sodium Starch Glycolate Compared Between the Nitrogen Adsorption Method and the Differential Scanning Calorimetry Thermal Method*

Material	N_2 Pore Radius† Mean; 95% Range‡ (nm)	DSC Thermal Porosity Analysis		Deviation (%)
		Monolayer Thickness (β) § (nm)	Adjusted DSC Pore Radius ‖ Mean; 95% Range‡ (nm)	
CCS	2.03; .81-5.06	0.46	2.13; 1.46-3.12	+4.92
SSG	2.99; .91-9.23	1.28	3.10; 2.35-4.09	+3.68

*CCS indicates croscarmellose sodium; DSC, differential scanning calorimetry; RH, relative humidity; and SSG, sodium starch glycolate.
†The nitrogen porosity distribution was obtained from the method based on the area of the pore walls utilized with Kelvin equation in adsorption path.
‡Either resulting differential nitrogen volume (d*V*/d*r*) in the nitrogen adsorption method or partial Gibb's free energy with corresponding radius in the thermal method was nonlinearly fitted into the following function:

$f = A \cdot exp\left[-0.5(ln\frac{r}{\bar{r}})/b)^2\right]$, where $\bar{r}$ and b are mean radius and the logarithmic value of distribution half-width, respectively. The distribution width is the value of exp(−b) + exp(+b). And, taking as logarithmic-normal distribution, the limits of 95% population range can be calculated as follows: $exp\left[ln(\overline{r_p}) \pm Z_{0.95} \cdot b\right]$.

§Monolayer thickness (β) is F_s X σ, where F_s and σ are swelling factor (1.6 and 4.4 for CCS and SSG, respectively[4]) and mean water molecule diameter[17] (.29 nm), respectively.
‖Adjusted pore radius is calculated as $r_k + \beta$, where β is monolayer thickness.

with those from nitrogen adsorption. Good agreement between the mean values of radii of 2 methods was found with less than 5% deviation.

It was found also that the porosity distribution obtained from sorbed water crystallization was considerably narrower than that from nitrogen adsorption (**Table 3**). The discrepancy may be attributed to a number of reasons: (1) Water molecules possessing hydrogen bonding may undergo volume contraction when condensed compared with nitrogen, which might misleadingly present narrower distribution. (2) On one hand, porosity distribution from nitrogen adsorption is not only dependent on Kelvin's equation but also on "nitrogen film" lying progressively inside pore radii with altering relative pressure during the process

of determination. With the used model, the pore size is very sensitive to film thickness calculation. (3) On the other hand, the limitations of porosity distribution from the DSC exotherm might be because the method is highly dependent on a number of assumptions, including the following:

- Only water capillary condensation is considered to be freezable.
- The exotherm was only referred to crystalline ice.
- DSC was run under nonequilibrium conditions.
- A portion of amorphous water may present, thus previous thermal history might affect the obtained pore size distribution.
- The relationship between radius and Gibb's free energy hold throughout the porosity range via Kelvin's equation.
- And nonfreezable bound water forms a swelling monolayer that lies along the inner pore surface, which might not only contribute to the pore radii but also to narrowing distribution.

In addition, the method of adjusting pore size discussed previously was static and based on uniform swelling that might not be adequately appropriate. It has been recognized that water sorption is dynamic. During sorption, water plasticization increases segmental mobility of polymer sorbent that in turn changes the structure of polymer. The situation, however, is not truly equilibrium. And, because glass transition temperature (T_g) of polymer sorbent decreases during the process, the conditions are not even isothermal with respect to the difference between experimental temperature and T_g.

CONCLUSION

It seems that the porosity determination by the DSC technique is successful but only in cases of CCS and SSG with 100% RH equilibration. It is noted that the method is highly dependent on a number of factors, such as the nature of sorbed water (ie, freezable/nonfreezable bound water), swelling due to hydration, the ability to crystallize loosely bound water, the nature of porosity of the surface, and the set conditions of the DSC experiment. Further study should be done to overcome the limitations discussed above and to extend the applicability to other hydrophilic surfaces.

ACKNOWLEDGEMENTS

The authors are very much indebted to School of Pharmacy, Purdue University, West Lafayette, IN, for providing an automatic surface area analyzer to complete the study. Special thanks also go to Faculty of Pharmaceutical Sciences, Prince of Songkla University, Hat Yai, Thailand for the remainder of laboratory supports.

REFERENCES

1. Sair L, Fetzer WR. Water sorption by starches. *Ind Eng Chem*. 1944;36:205-208.

2. Higuchi A, Iijima T. DSC investigation of the states of the water in poly(vinyl alcohol) membranes. *Polymer*. 1985;26:1207-1211.

3. Zografi G, Kontny MJ. The interactions of water with cellulose- and starch-derived pharmaceutical excipients. *Pharm Res*. 1986;3(4):187-194.

4. Stern SA, Saxena V. Concentration-dependent transport of gases and vapors in glassy polymers. *J Membr Sci*. 1980;7:47-59.

5. Mauze GR, Stern SA. The solution and transport of water vapor in poly(acrylonitrile): a re-examination. *J Membr Sci*. 1982;12:51-64.

6. Faroongsarng D, Peck GE. The swelling and water uptake of tablet III: moisture sorption behavior of tablet disintegrants. *Drug Dev Ind Pharm*. 1994;20(5):779-798.

7. Aharoni C. The solid-liquid interface in capillary condensation-sorption of water by active carbon. *Langmuir*. 1997;13:1270-1273.

8. Faroongsang D. The role of water sorption and swelling by an insoluble tablet containing cellulose, starch, or their derivative as a disintegrant during aqueous coating simulation [dissertation]. West Lafayette, IN: Purdue University, 1993:134-139.

9. Cuperus FP, Bargeman D, Smolders CA. Critical points in the analysis of membrane pore structures by thermoporometry. *J Membr Sci*. 1992;66:45-53.

10. Filho GR, Bueno WA. Water states of Cuprophan (hemodialysis membrane). *J Membr Sci*. 1992;74:19-27.

11. Young JH, Nelson GL. Theory of hysteresis between sorption and desorption isotherms in biological materials. *Trans Amer Soc Agric Eng*. 1967;10:260-263.

12. Ishikiriyama K, Todoki M. Pore size distribution measurements of silica gels by means of differential scanning calorimetry. *J Colloid Interface Sci*. 1995;171:103-111.

13. Ishikiriyama K, Sakamoto A, Todoki M, Tayama T, Tanaka, K, Kobayashi T. Pore size distribution measurements of polymer hydrogel membranes for artificial kidneys using differential scanning calorimetry. *Thermochim Acta*. 1995;267:169-180.

14. Hay JN, Laity PR. Observations of water migration during thermoporometry studies of cellulose films. *Polymer*. 2000;41:6171-6180.

15. Adamson WA. Capillary condensation. In: *Physical Chemistry of Surfaces*. 5th ed. New York, NY: John Wiley & Sons; 1990:661-666.

16. Flory PJ. Partial molar quantities. In: *Principle of Polymer Chemistry*. Ithaca, NY: Cornell University Press; 1953: 511-518.

17. Van Dooren AA, Muller BW. Purity determinations of drugs with differential scanning calorimetry (DSC)-a critical review. *Int J Pharm*. 1984;20:217-233.

18. Gregg SJ, Sing KSW. Use of the Kelvin equation for calculation of pore size distribution. In: *Adsorption, Surface Area and Porosity*. New York, NY: Academic Press; 1982:136-138.

19. Ping ZH, Nguyen QT, Chen SM, et al. States of water in different hydrophilic polymers-DSC and FTIR studies. *Polymer*. 2001;42:8461-8467.

20. Westermarck S. Use of Mercury Porosimetry and Nitrogen Adsorption in Characterisation of the Pore Structure of Manitol and

Microcrystalline Cellulose Powders, Granules, and Tablets [dissertation]. Helsinki, Finland: University of Helsinki; 2000.

21. Ozeki S. Dielectric properties of water adsorbed in slitlike micropores of jarosite. *Langmuir*. 1989;5:181-186.